Use of a Velocity Command Motor as a Reaction Mass Actuator

Jeffrey L. Sulla*
Lockheed Engineering and Sciences Company, Hampton, Virginia 23665
and
Jer-Nan Juang† and Lucas G. Horta‡
NASA Langley Research Center, Hampton, Virginia 23665

This paper presents results of a test application of a commercially available linear step motor as a reaction mass actuator. The system equations with velocity command actuator dynamics are derived. Differences between a velocity command actuator and a force command actuator are discussed. A beam structure and the NASA Mini-Mast were used for vibration suppression experiments. Simulation results and analysis including filter dynamics are given to verify the experimental performance in terms of transient responses and augmented damping level.

Introduction

THE development of linear force actuators has received much attention in recent years in support of vibration suppression of large space structures.[1,2] The linear force actuator consists of a reaction mass and a finite length track. The reaction mass can be controlled by a command to move in either direction along the track, with the resulting reaction force acting on the structure. In this paper, the application of an industrial linear step motor as a linear reaction mass force actuator operating in the relative velocity command mode is described.[3] Linear step motors have been widely used for precise position control of industrial processes. Some examples of use would be *X-Y* positioning tables and cut-to-length manufacturing processes.

The objective of this paper is to study the feasibility of using a velocity commanded linear step motor[4] for control of flexible structures. The approach is to use the step motor attached to a simple cantilevered beam and the NASA Mini-Mast and to perform theoretical analyses to verify the experimental results from different output feedback configurations. Output signals from beam acceleration, reaction mass acceleration, and root strain are used in the feedback loop, including the reaction mass relative position. Mini-Mast tip displacement is used in the feedback loop for Mini-Mast tests. Analytical and experimental results with different output signals in the feedback loop are shown and compared. The merits of using a velocity command actuator will be identified and discussed in comparison with a force command actuator. The outline of this paper includes test configuration description, theoretical analysis, experimental and numerical results, and concluding remarks.

Test Configuration Description

The test configuration is described as follows, including actuator description, test setup, and test software description.

A. Actuator Description

The basic configuration of a hybrid linear step motor is shown in Fig. 1. In a typical industrial application, the moving portion of the motor is the forcer and the stationary portion is the platen. The forcer contains two electromagnets and a permanent magnet. The platen is a passive element with teeth cut into its surface over which the bearing-supported forcer rides. Since the pole faces of the forcer and the teeth of the platen are in spatial quadrature, proportioning the current to the motor windings causes magnetic flux paths to be established that cause the forcer teeth to align with a set of the platen teeth, thereby causing motion between the two elements of the motor.

The linear motor used in this application was a Compumotor L5A manufactured by the Parker Hannifin Corporation. The motor has a static force capability of 6.0 lb (26.6 N) and has a 13.5 in. (34.3 cm) platen. The platen has 100 teeth per inch engraved in its surface to provide the pole faces for the forcer. The maximum operational step resolution is 12,500 steps per inch. In this application as a linear force actuator, the motor was mounted such that the platen was the moving element (the reaction mass) and the forcer was attached to the test structure. The weight of the platen is 3.5 lb (15.5 N) and that of the forcer is 0.8 lb (3.55 N).

The drive unit is an L series drive that is packaged with the motor from the Parker Hannifin Corporation. The L drive is a bipolar, microstepping drive specifically designed for two-phase, permanent-magnet, hybrid linear motors. The high step resolution of the linear motor is obtained by the drive unit digitally proportioning the current to the motor. In this application, 125 microsteps per platen tooth corresponds to an equivalent step motor resolution of 12,500 steps per inch.[5]

The indexer used to control the linear motor is a Compumotor PC23 microprocessor-based three-axis indexer that is inserted into a PC-AT expansion card slot. The PC23 provides the step pulses to the motor drive unit in response to user

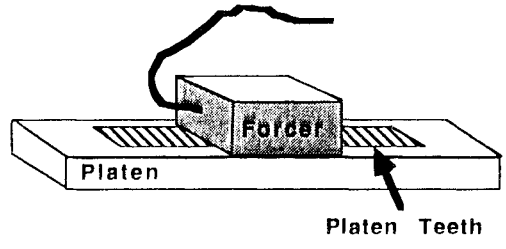

Fig. 1 Linear step motor configuration.

Presented as Paper 90-1227 at the AIAA Dynamic Specialist Conference, Long Beach, CA, April 5-6, 1990; received Aug. 15, 1990; revision received Dec. 10, 1990; accepted for publication Dec. 14, 1990.

*Senior Engineer.
†Principal Scientist, Spacecraft Dynamics Branch, MS 230. Fellow AIAA.
‡Aerospace Engineer, Spacecraft Dynamics Branch, MS 230. Member AIAA.

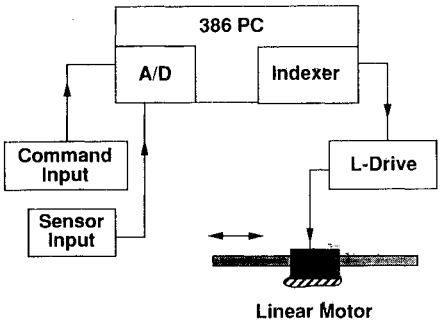

Fig. 2 Actuator system hardware interfaces.

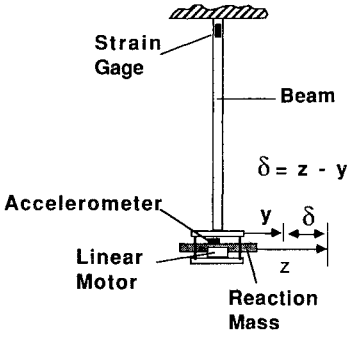

Fig. 3 Test beam.

inputs. A motion control mode defined as "velocity streaming" is used to provide real-time control of the linear motor velocity. In the velocity streaming mode, motor velocity can be changed in increments of approximately 15.3 motor steps per second. For these tests this corresponds to a velocity command increment of 0.00122 in./s. Software execution speed determines the command update rate (or frame rate) in the absence of a real-time clock system.[6]

B. Test Setup

The linear motor was tested bench mounted (forcer was fixed) and also attached to a simple beam structure and the NASA Mini-Mast for closed-loop performance tests. A PC-based data acquisition system with analog to digital (A/D) converters was used to obtain real-time sensor data such as acceleration (of the reaction mass or beam), beam strain gauge output, or Mini-Mast displacement sensor outputs. A high-precision low-pass filter was used on the accelerometer output before the A/D converter. Figure 2 depicts the actuator system hardware interfaces.

The beam structure used as the first test article for the closed-loop tests was a vertically cantilevered aluminum tube (beam) with an actuator mounting plate to which the linear step motor was attached. The structure with the linear motor attached has a first bending mode at 1.812 Hz and an open-loop damping of 0.07%. The mass of the beam is approximately five times that of the reaction mass (see Fig. 3). The second test article used was the NASA Mini-Mast,[7] which is a 20-m vertically cantilevered near-flight quality truss beam. For these tests, two linear motors were used to provide two axis control. The linear motors were mounted on the tip plate to provide control forces along the Mini-Mast global bending axis. The first five modes of the Mini-Mast are as follows: first X and Y bending (0.85 Hz), first torsion (4.2 Hz), and second coupled X and Y bending (6.2 Hz).

C. Test Software Description

The host computer communicates with the PC23 indexer via ASCII character strings written to and read from the indexer using the indexer command format. These ASCII characters are written to and read one at a time from registers at the base address of the indexer. In this application, software drivers provided with the indexer for command read and write were converted to C programming language for inclusion in the test software used for open-loop and closed-loop testing.

The open-loop test software requirements were to reset the indexer, allow input of excitation command parameters, enter velocity streaming mode, output commands to the motor, and exit velocity streaming mode. Command update rates of up to 250 Hz were obtained.

The beam closed-loop test software required additional routines to read the A/D converter and read reaction mass relative position from the PC23 indexer. These routines along with control of the excitation, free decay, and closed-loop phases of the experiment resulted in a decrease in the frame rate to 55 Hz (with 80386 PC), which still allowed smooth motor operation. Routines were also added to allow the saving of reaction mass relative position and accelerometer or strain gauge data for postprocessing.

Mini-Mast test software required the ability to operate two linear motors independently, along with acquiring three displacement sensor signals and reading the reaction mass relative position of the two actuators. The overhead associated with the additional indexer operations required for using two linear motors reduced the frame rate to 23 Hz, which was still adequate for testing on the first bending mode of the Mini-Mast.

Theoretical Analysis

This section includes the derivation of general equations of motion for flexible structures, actuator dynamics with a velocity command, and filter dynamics. The measured output signals include acceleration and structural deflection (or strain). These formulations are used to develop feedback configurations for the test setup described earlier. From an analytical point of view, differences between a velocity-commanded actuator and a force-commanded actuator are shown and discussed. The effects of the phase shift due to the filter dynamics on the feedback control loop are also discussed.

Consider the system, shown in Fig. 3, which consists of an aluminum beam fixed at one end and a reaction mass actuator attached at the other end. Let $y^T = [y_1, y_2, \ldots, y_n]$ be the deflection vector of the beam, M_b the $n \times n$ mass matrix of the beam, K_b the $n \times n$ stiffness matrix of the beam, z_n the displacement of the reaction mass, and m_n the reaction mass. The subscript n means that the associated quantity is related to the coordinate n. The equation of motion is then written as

$$M_b\ddot{y} + K_b y = -b_n m_n \ddot{z}_n \tag{1}$$

where $b_n = [0, 0, \ldots, 1]^T$ and y_n equals the location of the reaction mass. It should be noted that $y_n = b_n^T y$.

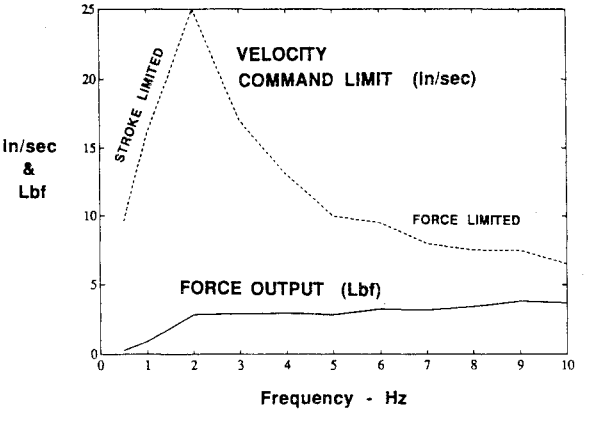

Fig. 4 Actuator velocity command limits.

A. Direct Output Feedback Without Filtering

The reaction mass relative velocity is expressed by

$$\dot{\delta}_n = \dot{z}_n - \dot{y}_n \tag{2}$$

and let the output feedback command to the actuator be

$$\dot{\delta}_n = -G_{na}\ddot{z}_n + G_{ny}y_n - G_{nd}\delta_n \tag{3}$$

Obviously, δ_n is the relative displacement of the reaction mass with respect to the tip of the beam. It is assumed in Eq. (3) that the input command to the actuator is identically equal to the relative velocity. This assumption holds only if the commands are kept within the step motor limitation. The reaction mass acceleration $\ddot{z}_n$ is measured by an accelerometer and the relative displacement δ_n is obtained by counting steps of the reaction mass position that are provided by the motor indexer. Since the tip deflection of a cantilevered beam is proportional to its strain, a strain gauge located at the root of the beam is used to derive tip deflection measurement. The gains G_{na}, G_{ny}, and G_{nd}, respectively, for $\ddot{z}_n$, y_n, and δ_n are determined by the control performance requirements for the system, such as the decay rate of vibration suppression. It should be noted that the signs for the gains G_{ny} and G_{na} in Eq. (3) are different to reflect that phases for the acceleration and displacement are 180 deg apart for a system with no damping. There are many other measured signals that may be used in Eq. (3) for control feedback. Here, the reaction mass acceleration, the tip deflection, and the reaction mass relative displacement are chosen because the sensors to measure these quantities are readily available.

The actuator is commanded in such a way that the reaction mass moves with the speed $\dot{\delta}_n$, in contrast with the conventional force or displacement commanded reaction mass actuators. The differences between the velocity command and the force command are discussed in the sequel. Multiplying Eq. (3) by m_n/G_{na} for the case where $G_{na} \neq 0$ and combining the result with Eq. (1) yields the following matrix equation:

$$M_t\ddot{y}_t + D_t\dot{y}_t + K_t y_t = 0 \tag{4}$$

where

$$M_t = \begin{bmatrix} M_b + b_n b_n^T m_n & b_n m_n \\ b_n^T m_n & m_n \end{bmatrix}$$

$$D_t = \begin{bmatrix} 0 & 0 \\ 0 & m_n/G_{na} \end{bmatrix}$$

$$K_t = \begin{bmatrix} K_b & 0 \\ -b_n^T(m_n/G_{na})G_{ny} & (m_n/G_{na})G_{nd} \end{bmatrix}$$

$$y_t = \begin{bmatrix} y \\ \delta_n \end{bmatrix}$$

The equality $y_n = b_n^T y$ has been used in deriving Eq. (4). Matrix M_t in Eq. (4) is positive definite and D_t is positive semidefinite if G_{na} is positive definite, i.e., $G_{na} > 0$.

For the case where $G_{ny} = 0$, i.e., no tip deflection feedback, matrix K_t is positive definite if $G_{na} > 0$ and $G_{nd} > 0$, since K_b is positive definite for a cantilevered beam. In this case, it is known that the system, Eq. (4), is stable. In other words, a velocity command actuator will provide a stable closed-loop system without any velocity feedback [see Eq. (3)]. Reaction mass acceleration feedback in combination with relative displacement feedback is sufficient to augment structural damping when using a velocity command actuator.

For the case where the acceleration feedback is absent, $G_{na} = 0$, Eq. (3) becomes

$$\dot{\delta}_n = G_{ny}y_n - G_{nd}\delta_n \tag{5}$$

Differentiating Eq. (5) once with respect to time t and combining the resulting equation with Eqs. (1) and (2) gives

$$(M_b + b_n b_n^T m_n)\ddot{y} + b_n b_n^T m_n G_{ny}\dot{y} - b_n m_n G_{nd}\dot{\delta}_n + K_b y = 0 \tag{6}$$

It is obvious that if $G_{nd} = 0$ and $G_{ny} > 0$, Eq. (6) is stable. As a result, a velocity command actuator may augment structural damping by using deflection feedback. The relative displace-

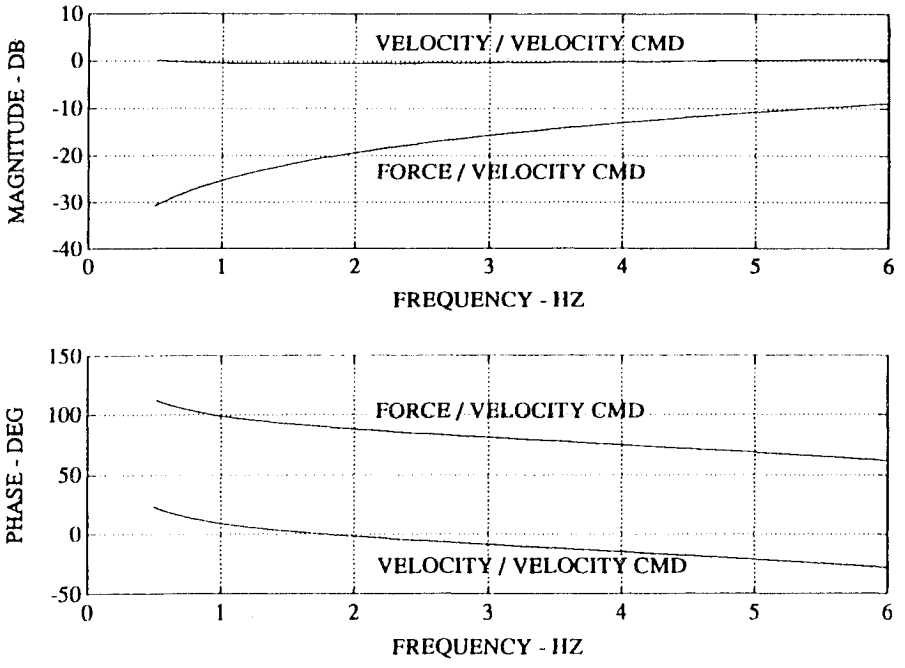

Fig. 5 Actuator frequency response—force/velocity command, reaction mass velocity/velocity command.

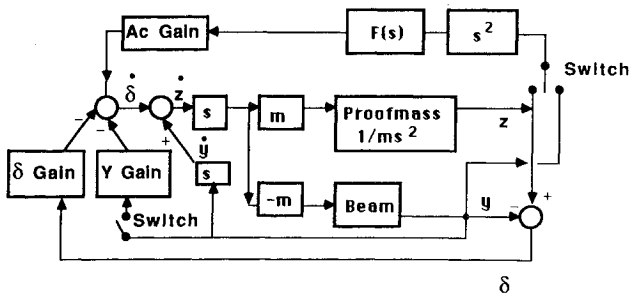

Fig. 6 Beam closed-loop system.

ment feedback of the reaction mass acts as a spring that keeps the reaction mass centered, whereas the beam deflection feedback provides the damping for the system. The conventional approach requires a velocity measurement to augment the system damping. The beam deflection may be characterized by a strain gauge located at the root of the beam.

For simulation, Eqs. (5) and (6) can be combined into the following equation:

$$\begin{bmatrix} M_b + b_n b_n^T m_n & 0 & -b_n m_n G_{nd} \\ 0 & I & 0 \\ 0 & 0 & 1 \end{bmatrix} \begin{bmatrix} \ddot{y} \\ \dot{y} \\ \dot{\delta}_n \end{bmatrix}$$

$$+ \begin{bmatrix} b_n b_n^T m_n G_{ny} & K_b & 0 \\ -I & 0 & 0 \\ 0 & -b_n^T G_{ny} & G_{nd} \end{bmatrix} \begin{bmatrix} \dot{y} \\ y \\ \delta_n \end{bmatrix} = 0 \tag{7}$$

Since Eq. (7) does not contain the acceleration $\ddot{\delta}_n$, it has an odd number of closed-loop states, which implies that there always exists at least an overdamped eigenvalue, if the closed-loop system is stable. The difference between Eq. (4) and Eq. (7) becomes obvious since Eq. (4) has the acceleration $\ddot{\delta}_n$ involved that makes it possible to write Eq. (4) in terms of a second-order equation. In other words, Eq. (4) has an even number of closed-loop states that may not possess an overdamped eigenvalue.

B. Direct Output Feedback with Filtering

The motion of a linear step motor is piecewise continuous. This discontinuity in motion introduces high frequency components into the accelerometer signal. The effect of high frequency on the feedback control is reduced by using low-pass filters. Let the acceleration signals be filtered such that

$$\dot{x}_f = A_f x_f + B_f \ddot{z}_n \tag{8}$$

$$z_f = C_f x_f \tag{9}$$

where the quantity z_f is the filtered signal obtained from the measured acceleration $\ddot{z}_n$. The filter dynamics are described by the filter state matrix A_f, the filter input influence matrix B_f, the filter output influence matrix C_f, and the filter state vector x_f. The filter is used in cleaning up the measured signals.

Let the actuator be commanded such that the relative velocity of the reaction mass is

$$\dot{\delta}_n = -G_{na} z_f - G_{nd} \delta_n \tag{10}$$

where z_f is the filtered signal obtained from Eqs. (8) and (9). Solving for $\ddot{z}_n$ from Eq. (2) and for $\dot{\delta}_n$ from Eq. (10) and substituting the resulting equation into Eqs. (1), (8), and (9), one obtains the following equations:

$$(M_b + b_n b_n^T m_n)\ddot{y} + K_b y - b_n m_n [G_{na} C_f \dot{x}_f + G_{nd} \dot{\delta}_n] = 0 \tag{11}$$

$$\dot{\delta}_n + G_{na} C_f x_f + G_{nd} \delta_n = 0 \tag{12}$$

$$\dot{x}_f - A_f x_f - B_f b_n^T \ddot{y} + B_f [G_{na} C_f \dot{x}_f + G_{nd} \dot{\delta}_n] = 0 \tag{13}$$

or in matrix form we have

$$\begin{bmatrix} M_b + b_n b_n^T m_n & 0 & -b_n m_n G_{nd} & -b_n m_n G_{na} C_f \\ 0 & I & 0 & 0 \\ 0 & 0 & 1 & 0 \\ -B_f b_n^T & 0 & B_f G_{nd} & I + B_f G_{na} C_f \end{bmatrix} \begin{bmatrix} \ddot{y} \\ \dot{y} \\ \dot{\delta}_n \\ \dot{x}_f \end{bmatrix}$$

$$+ \begin{bmatrix} 0 & K_b & 0 & 0 \\ -I & 0 & 0 & 0 \\ 0 & 0 & G_{nd} & G_{na} C_f \\ 0 & 0 & 0 & -A_f \end{bmatrix} \begin{bmatrix} \dot{y} \\ y \\ \delta_n \\ x_f \end{bmatrix} = 0 \tag{14}$$

To make this system stable, the gains G_{na} and G_{nd} should be properly chosen such that Eq. (14) has eigenvalues with negative real parts. The stability margins for the gains G_{na} and G_{nd} depend on the filter dynamics characterized by the matrices A_f, B_f, and C_f. Obviously, the coupling of filter dynamics cannot be ignored in a closed-loop control design. Indeed, the coupling of filter dynamics is as important as the actuator dynamics. Note that, in some cases, the number of filtered states may be more than the number of combined actuator and system states.

Although the equations of motion presented in this section are based on a single actuator, they can be easily extended for multiple actuators.

Experimental and Numerical Results

A. Actuator Characteristics

General operating characteristics of the linear motor operating in the velocity streaming mode were determined when tested bench mounted. In Fig. 4, the maximum sinusoidal velocity command operating limits with the corresponding derived force were plotted. These limits were determined by commanding various sinusoidal velocity commands and observing the effect of increasing amplitude and frequency on the motor performance. The limits indicated correspond to either a lack of stroke for the commanded motion (at low frequencies) or force saturation characterized by motor stall/slip (at higher frequencies). With high motor command update rates, the linear motor exhibited smooth performance. From Fig. 4, it can be seen that the maximum force available at the first mode frequency of the test beam is approximately 2.3 lb (10.23 N). By using a spare A/D channel to input an analog command to the linear actuator system, a dynamic signal analyzer was used to perform a sine sweep test from 0.5 to 6 Hz. An accelerometer mounted on the reaction mass was

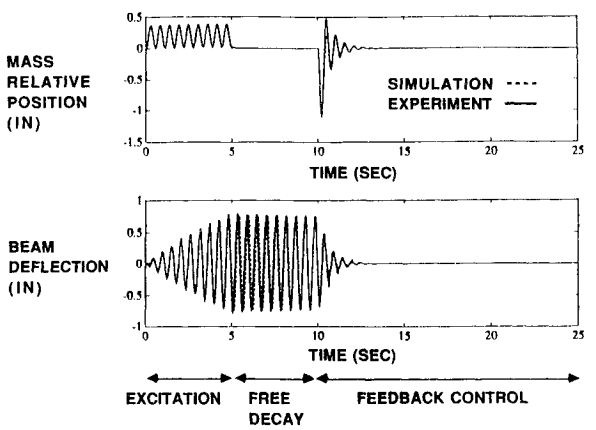

Fig. 7 Beam strain gauge and relative position feedback.

used to obtain a frequency response (Fig. 5) between velocity command and actuator force output. In the frequency range of the first bending modes of the test articles, the actuator has 90–100 deg of phase shift between velocity command and force output. The magnitude plot agrees well with the calculated available force level shown in Fig. 4. A derived velocity command to reaction mass relative velocity frequency response is also shown on Fig. 5, which shows a flat magnitude response from 0.5 to 6 Hz.

B. Comparison of Beam Test Results

Three types of beam output feedback for structural damping augmentation were demonstrated in these closed-loop tests. Reaction mass acceleration, beam acceleration, and beam root strain gauge outputs were used as the feedback signals. Reaction mass relative position feedback was used to insure that the reaction mass remained centered during the closed-loop phase. The reaction mass relative position was obtained from the PC23 indexer that maintained a count of motor step pulses sent to the motor that corresponded to the actual motion of the platen (as long as the motor had not stalled or slipped).

The closed-loop beam tests were composed of three phases. The first phase was 5 s of sinusoidal excitation at the first mode resonant frequency followed by 5 s of zero excitation command with relative position feedback to return the reaction mass to the center reference position. The reaction mass actuator introduced no inadvertent damping to the system with a zero relative velocity command. At 10 s, the damping augmentation loop was closed using either reaction mass acceleration, beam acceleration, or beam root strain gauge output and reaction mass relative position to generate the actuator velocity command to damp the beam vibration and keep the reaction mass centered. The total test time was 25 s.

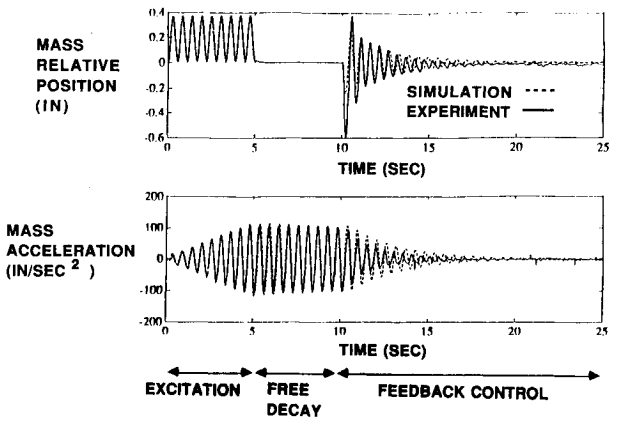

Fig. 8 Reaction mass acceleration and relative position feedback.

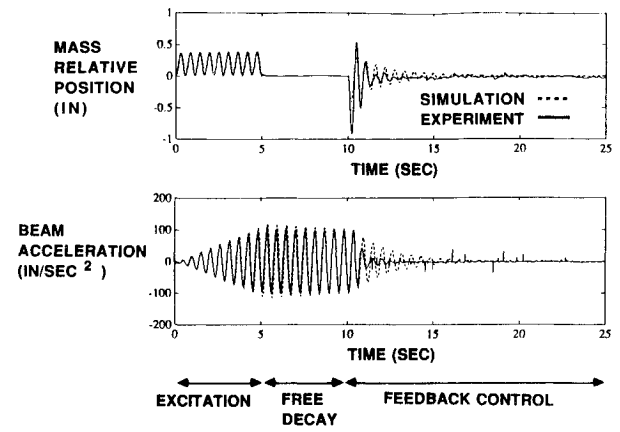

Fig. 9 Beam acceleration and relative position feedback.

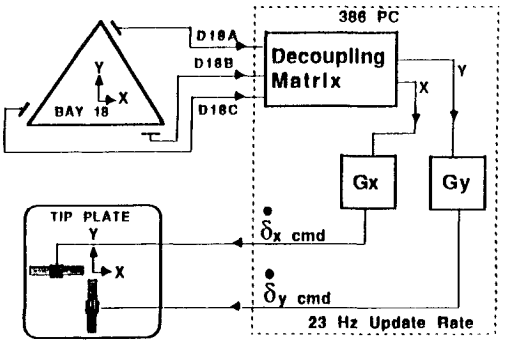

Fig. 10 Mini-Mast feedback loops.

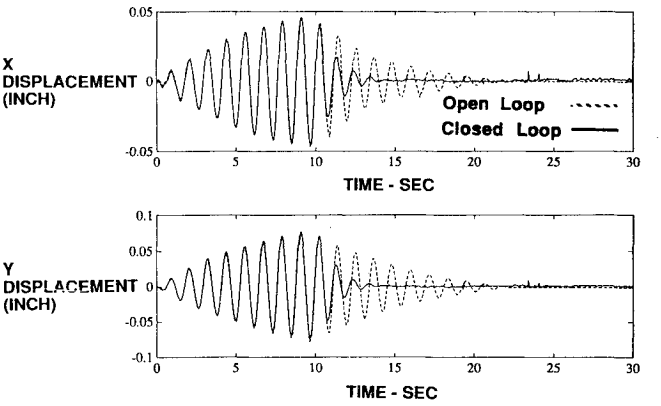

Fig. 11 Mini-Mast experimental results.

An overall block diagram of the closed-loop systems tested is shown in Fig. 6. For each closed-loop experiment, the indicated switches determine the feedback signal used to augment the beam damping. For the beam experiments, $G_{nd} = 4$ s^{-1}, $G_{ny} = 21.97$ s^{-1}, $G_{na} = 0.047$ s, and beam acceleration gain = 0.079 s.

In Fig. 7, experimental (solid lines) and simulated (dashed lines) results are shown for the strain gauge and relative position feedback case. In this test, a closed-loop damping of 14.5% was achieved. Simulated closed-loop results were obtained using Eq. (7). The experimental results were obtained without any filtering of the strain gauge output.

Figure 8 shows experimental and simulated results for filtered reaction mass acceleration and relative position feedback. The closed-loop experimental results indicate more damping in the system than simulated output using Eq. (14). In this case, the accelerometer output was filtered through two Butterworth filters in series with a cutoff frequency set to 6 Hz.

Experimental and simulated results for the case of filtered beam acceleration and reaction mass relative position feedback are shown in Fig. 9. The experimental closed-loop damping appears to be much greater than that predicted by the numerical simulation results obtained using Eq. (14) with a slight modification. Intuitively, one would expect closed-loop damping comparable to that achieved via strain gauge (or deflection) feedback by only changing the sign of the feedback gain, assuming acceleration is 180 deg out of phase with the beam displacement (with no damping). However, the coupling of the reaction mass relative acceleration in Eq. (4) indicates that the system may be unstable. The experimental results with the filtered beam acceleration show that in this case the influence of the relative acceleration of the reaction mass is not significant enough to make the system unstable. In fact, the closed-loop damping in this case approaches that using displacement feedback (see Fig. 6). The filter dynamics make the closed-loop system stable.

C. Comparison of Mini-Mast Test Results

Figure 10 depicts the Mini-Mast tip displacement feedback loops that were implemented. For clarity, the reaction mass relative position feedback loops (with $G_{nd} = 1.0\ s^{-1}$) are not shown. Mini-Mast tip deflection detected by three noncontacting displacement probes were input to the 80386 PC system. The displacement inputs were multiplied by a geometric decoupling matrix to obtain centroidal displacement of the Mini-Mast tip plate with respect to the global bending axis. These global X and Y displacements were multiplied by their respective gains ($G_x = G_y = 70\ s^{-1}$) to generate the corresponding reaction mass actuator relative velocity command. The frame cycle for this process was 23 Hz.

Figure 11 shows typical experimental results. The Mini-Mast was excited for 9.8 s at the first bending mode frequency (0.85 Hz) with both reaction mass actuators, followed by the feedback control at 10 s. The structural damping was increased from the 4.5% free decay damping to approximately 15% with displacement feedback.

Concluding Remarks

In this paper, it has been demonstrated that an industrial linear step motor system can be used as a reaction mass actuator for control of a flexible structure. Results show achievable damping levels from both analysis and experiments. The analytical studies that are motivated by experimental results yield general formulations for output feedback with a velocity command actuator. The use of relative velocity command allows damping augmentation without a velocity sensor in the feedback loop. Instead, displacement or acceleration sensor outputs can be used. In contrast, when using a force command actuator, the output signals from position or acceleration may be filtered to approximate the velocity phase for damping augmentation. The additional filter dynamics may cause system instability. Without filter dynamics in the feedback loop, it can be concluded that a velocity command actuator requires output signals from acceleration or displacement, whereas a force command actuator requires output signals from velocity to augment the structural damping.

References

[1]Politansky, H., and Pilkey, W. D., "Suboptimal Feedback Vibration Control of a Beam with a Proof-Mass Actuator," *Journal of Guidance, Control, and Dynamics,* Vol. 12, No. 5, 1989, pp. 691–697.

[2]Zimmerman, D. C., Inman, D. J., and Horner, G. C., "Dynamic Characterization and Microprocessor Control of the NASA/UVA Proof-Mass Actuator," AIAA Paper 84-1077, May 1984.

[3]Aubrun, J. N., and Margulies, G., "Low-Authority Control Synthesis for Large Space Structures," NASA CR-3495, Sept. 1982.

[4]Lange, T., "Investigation of Flight Sensors and Actuators for the Vibration Suppression Augmentation of Large Flexible Space Structures," European Space Agency, ESA CR(P)-2670, Paris, France, May 1988.

[5]"Compumotor Operator's Manual PC23 P/N:88-007015-03," Parker Hannifin Corporation, Petaluma, CA, 1988.

[6]"L Series User Guide P/N 88-007753-01," Parker Hannifin Corporation, Petaluma, CA, Aug. 31, 1988.

[7]Pappa, R. S., Schenk, A., and Noll, C., "ERA Modal Identification Experiences with Mini-Mast," 2nd USAF/NASA Workshop on System Identification and Health Monitoring of Precision Space Structures, California Inst. of Tech., Pasadena, CA, March 27–29, 1990.